Non-DC-Biased OFDM with Optical Spatial Modulation

Yichen Li, Dobroslav Tsonev and Harald Haas

Institute for Digital Communications,
Joint Research Institute for Signal and Image Processing,
The University of Edinburgh,
EH9 3JL, Edinburgh, UK
Email: {yichen.li, d.tsonev, h.haas}@ed.ac.uk

***Abstract*—In this paper, a novel optical Orthogonal Frequency Division Multiplexing (OFDM) modulation approach is presented. This method uses the Optical Spatial Modulation (OSM) technique to obtain positive and real-valued signals which are required by an Optical Wireless Communication (OWC) system. In comparison to existing OFDM methods applied to the OSM system, the new scheme, Non-DC-biased OFDM (NDC-OFDM), has significant advantages. Compared to DC-biased Optical OFDM (DCO-OFDM), NDC-OFDM avoids DC-biasing and, thus, improves the power efficiency. Moreover, the spectral and power efficiency of the new approach are better than the well-known unipolar optical modulation scheme, Asymmetrically Clipped Optical OFDM (ACO-OFDM). The bit-error ratio (BER) performances of these three methods are compared. Compared to ACO-OFDM and DCO-OFDM, NDC-OFDM has an energy saving gain of at least 5 dB for the same spectral efficiency. The improvement comes at the expense of additional hardware at the transmitter and receiver. However, visible light communication (VLC) systems typically are equipped with multiple low-cost Light Emitting Diodes (LEDs) to fulfill minimum indoor lighting conditions.**

***Index Terms*—optical spatial modulation, optical OFDM, optical wireless communication, MIMO.**

I. Introduction

With the rapid increase in wireless services and applications, the limited radio frequency (RF) spectrum may not be sufficient to cope with future data rate demands. As a viable complementary approach, Optical Wireless Communication (OWC) has gained significant attention as a result of technological breakthroughs in solid state lighting technology [1]. The momentous advantage of OWC is that it offers a very large bandwidth for each transmitting LED.

In current OWC systems, Light Emitting Diodes (LEDs) are used as transmitters to convert the modulated electrical signal to an optical signal. At the receiver, the optical signal is detected by photodiodes (PDs) and demodulated using digital signal processing techniques. Off-the-shelf LEDs and PDs can be used to realize a low-cost visible light communication (VLC) system which can achieve high bit rates of at least 500 Mb/s [2]. However, LEDs disallow the use of phase information for data transmission. As a consequence, only real-valued and positive signals can be used for data modulation. This is in stark contrast to RF systems which make use of complex valued and bi-polar signals. Thus, OWC using incoherent light sources as described can only be realized as an intensity modulation (IM) and direct detection (DD) system [3]. For IM/DD, standard digital modulation techniques are conceived, such as On-Off Keying (OOK), Pulse Position Modulation (PPM) and Pulse Amplitude Modulation (PAM) [4].

For high-speed data transmission, Intersymbol Interference (ISI) becomes an issue and computationally complex equalization techniques are required. In the fourth-generation (4G) wireless communication, Orthogonal Frequency Division Multiplexing (OFDM) is used, as it is better equipped to handle severe ISI. In optical communications, OFDM can also be applied in the context of IM/DD systems [5]. Because the IM/DD system can only transmit real-valued signals, Optical OFDM (O-OFDM) needs to produce real-valued symbols. This can be achieved by imposing Hermitian symmetry on the information frame before the inverse fast Fourier transform (IFFT) operation during the signal generation phase. This comes at the expense of half of the spectral efficiency. In general, standard techniques to ensure positive optical signals, which are required by LEDs, are DC-biased Optical OFDM (DCO-OFDM) and Asymmetrically Clipped Optical OFDM (ACO-OFDM) [6][7]. In DCO-OFDM, a DC-bias is added. In ACO-OFDM, the system inserts zeros on even subcarriers and modulates only odd subcarriers. As a result, a group of antisymmetric real-valued OFDM symbols are obtained, as shown in [8]. This allows any negative samples to be clipped without distortion. DC-bias and clipping noise in DCO-OFDM have an impact on the bit-error ratio (BER) performance [9]. When high-power signals are required, the effect becomes significant. In ACO-OFDM, although there is negligible DC-bias, the scheme sacrifices 50% spectral efficiency compared to DCO-OFDM for the same Quadrature Amplitude Modulation (QAM) constellation size.

As introduced in this paper, the original O-OFDM modulator can be combined with Spatial Modulation (SM) [10] to result in a new method, Non-DC-biased OFDM (NDC-OFDM). This system inherits characteristics from SM (low complexity) and OFDM (ISI resistance). More importantly, it

978-1-4577-1348-4/13/$31.00 ©2013 IEEE

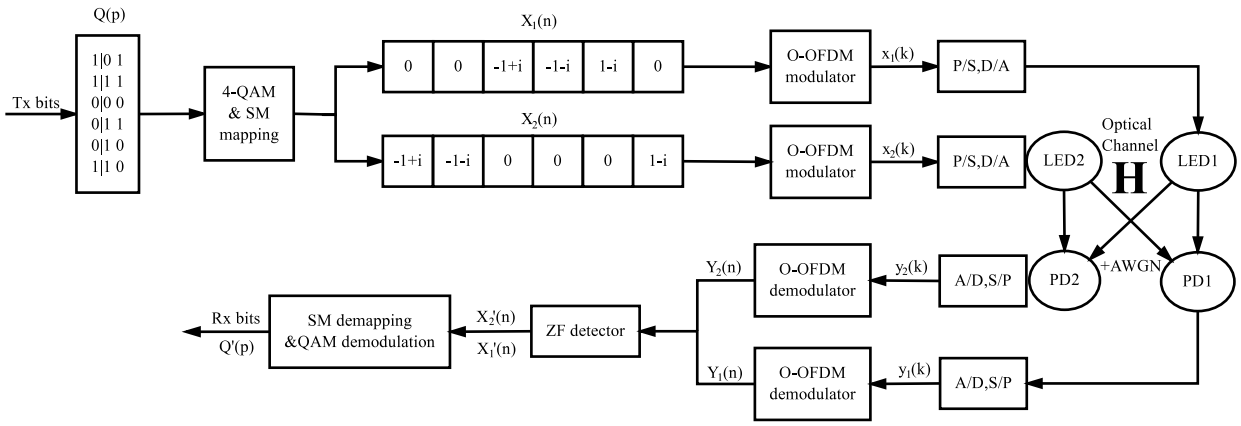

Fig. 1. Block diagram of the conventional OSM-OFDM system

solves the DC-bias problem in DCO-OFDM and has a higher spectral efficiency than ACO-OFDM.

The rest of this paper is organized as follows. The system model of traditional OSM combined with DCO-OFDM and ACO-OFDM is described in Section II. Section III presents the system model of NDC-OFDM. Section IV shows the result of a comparison between NDC-OFDM and conventional OSM-OFDM in terms of their BER performances, power efficiency and spectral efficiency. Finally, Section V concludes this paper.

II. Conventional OSM-OFDM System Model

Fig. 1 shows the system model of the conventional OSM-OFDM system. This system combines the basic SM-OFDM [10] and traditional O-OFDM techniques [6].

In the first step of the modulation procedure, the input bit stream is reshaped and placed in an $N \times m$ matrix, $\mathbf{Q}(p)$, where N is the number of OFDM subcarriers and $m = \log_2(MN_t)$. Moreover, M is the QAM constellation size and N_t denotes the number of transmitters. This paper compares NDC-OFDM with OSM-OFDM when N_t is set to two. Under this assumption, bits in the first column of $\mathbf{Q}(p)$ represent the index of transmitters. This means that when the bit in the first column is zero, the rest of the bits on the same row will be transmitted by the first LED and when it equals one, the rest of the bits will be conveyed by the second LED. Bits in the other columns of each row will be transformed to complex M-QAM symbols. For example, in Fig. 1, it can be seen that the first row of $\mathbf{Q}(p)$ is [1|0 1]. This means that [0 1] will be converted to a QAM symbol $-1+\mathrm{i}$ by Gray mapping and this symbol will be put in the first slot of $\mathbf{X}_2(n)$, as illustrated in Fig. 1. Simultaneously, the first slot of $\mathbf{X}_1(n)$ will be set to zero. As a result of the M-QAM and SM mapping, two complex vectors, $\mathbf{X}_1(n)$ and $\mathbf{X}_2(n)$, are obtained. Each vector passes through an O-OFDM modulator. In general, two standard techniques, ACO-OFDM and DCO-OFDM, are used to obtain positive and real-valued OFDM symbols, which are introduced and compared in [6] and [9]. In ACO-OFDM, $N/4$ QAM symbols are mapped onto half of the odd subcarriers of an OFDM frame. At the same time, the even subcarriers are set to zero. In DCO-OFDM, $N/2-1$ symbols are put into the first half of subcarriers and the DC subcarrier (the first subcarrier) is set to zero. Afterwards, for both ACO-OFDM and DCO-OFDM, Hermitian symmetry is applied on the rest of the OFDM frame. Thus, the two groups of QAM symbols from $\mathbf{X}_1(n)$ and $\mathbf{X}_2(n)$ are mapped onto OFDM frames and they are transformed into real-valued OFDM symbols by the IFFT block. Finally, in order to get positive symbols, the negative values need to be set to zero in ACO-OFDM. In DCO-OFDM, before clipping, a DC-biased power is added to the bipolar OFDM symbols.

The resulting output vectors at the O-OFDM modulator, $\mathbf{x}_1(k)$ and $\mathbf{x}_2(k)$, are transmitted by the respective LED over an $N_t \times N_r$ optical multiple-input multiple-output (MIMO) channel, $\mathbf{H}$, where N_r is the number of receivers. In this paper, the main objective is to compare the performance of the conventional OSM-OFDM system with NDC-OFDM. Therefore, the same optical channel is used for all three schemes. This channel is presented in Section III.

At the receiver, PDs convert optical signals to electrical signals. Additive white Gaussian noise (AWGN) is added to the signal due to ambient light and thermal noise in the transimpedance amplifier. Through the analog-to-digital conversion block, signals from each PD can be transferred to their corresponding vectors, $\mathbf{y}_1(k)$ and $\mathbf{y}_2(k)$. Each vector will be dealt with by the respective O-OFDM demodulator. As in conventional O-OFDM techniques, the received OFDM symbols are passed through a fast Fourier transform (FFT) operation which converts symbols to the frequency domain. In DCO-OFDM, $N/2-1$ symbols are obtained from the corresponding subcarriers and in ACO-OFDM, $N/4$ symbols are obtained. The extracted symbols are transferred to two complex vectors, $\mathbf{Y}_1(n)$ and $\mathbf{Y}_2(n)$. Zero forcing (ZF) is used to reverse the impairments of the MIMO channel to transform $\mathbf{Y}_1(n)$ and $\mathbf{Y}_2(n)$ into $\mathbf{X}_1'(n)$ and $\mathbf{X}_2'(n)$ respectively [10]. Afterwards, the SM detector compares the absolute values of the corresponding subcarriers from each channel to estimate

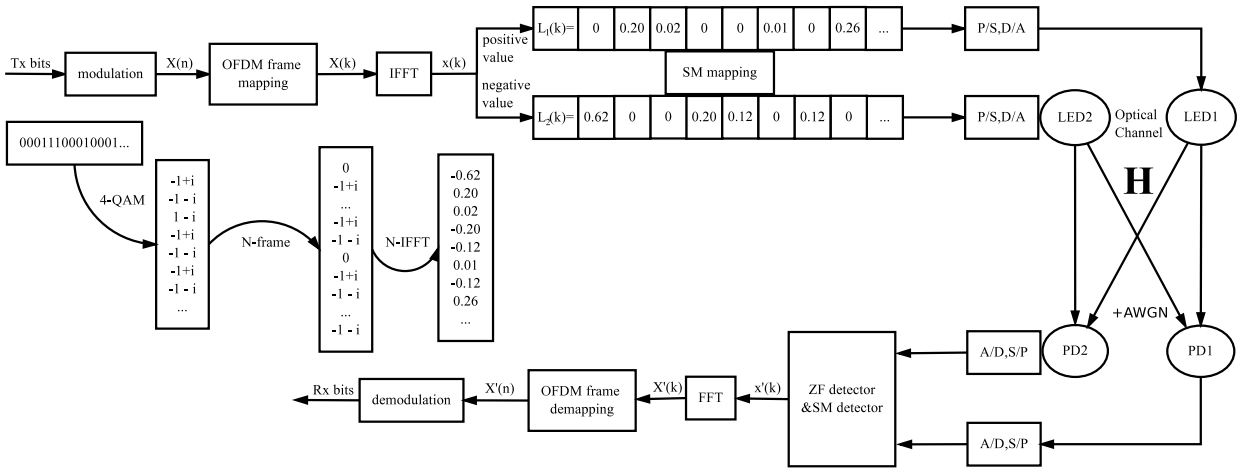

Fig. 2. Block diagram of the NDC-OFDM system

the indices of the active transmitters as follows,

$$\tilde{\mathbf{j}}(n) = \arg\max_{i}(|\mathbf{X}_i'(n)|), i = 1, \cdots, N_t, \tag{1}$$

As a result, the index of the estimated subchannel gives the bit information transmitted by the SM technique [10]. The bits from the estimated indices are put into the first column of the output matrix, $\mathbf{Q}'(p)$. This means that if $\tilde{\mathbf{j}}(n)$ is equal to one, the corresponding bit is zero and if the result of the estimation is two, the bit is one. At the same time, the largest symbol in each comparison is chosen as the detected symbol,

$$\mathbf{X}_d'(n) = \begin{cases} \mathbf{X}_1'(n), & \tilde{\mathbf{j}}(n) = 1, \\ \mathbf{X}_2'(n), & \tilde{\mathbf{j}}(n) = 2. \end{cases} \tag{2}$$

The detected QAM symbols are then decoded by the conventional Maximum Likelihood estimator. The result is allocated to the other columns of $\mathbf{Q}'(p)$. Finally, the output bit stream is obtained by reshaping $\mathbf{Q}'(p)$ into a serial bit stream. The described SM detection algorithm is not the optimal one according to [11]. However, it has been selected in this work for its low computational complexity.

III. NDC-OFDM System Model

The system model of NDC-OFDM is illustrated in Fig. 2. The input bit stream is transformed into complex symbols, $\mathbf{X}(n)$, $n = 1, \cdots, N/2 - 1$, by an M-QAM modulator. As in DCO-OFDM, $N/2 - 1$ QAM symbols are modulated onto the first half of an OFDM frame, $\mathbf{X}(k)$, $k = 1, \cdots, N$, and Hermitian symmetry is imposed on the second half of the OFDM frame. After the N-IFFT operation, the complex QAM symbols become N real-valued OFDM samples, $\mathbf{x}(k)$, but they are still bipolar.

In NDC-OFDM, LEDs only send the absolute value of $\mathbf{x}(k)$ and the sign of the symbol is represented by the index of the corresponding LED. According to the working principle of OSM, only one LED is activated during one symbol time. If the transmitted symbol is positive, the first LED will be activated to send the symbol. If the symbol is negative, its absolute value will be sent by the other LED. This principle constitutes the most significant difference between the traditional OSM-OFDM and the NDC-OFDM. An additional difference is that QAM symbols go through an OFDM modulator first and then pass through the SM mapping block in NDC-OFDM. In conventional OSM-OFDM, the order is reversed.

As shown in Fig. 2, after SM mapping, the converted optical signals, $\mathbf{L}_1(k)$ and $\mathbf{L}_2(k)$, will be transmitted by the corresponding LED over the optical MIMO channel $\mathbf{H}$ [12]. The $N_t \times N_r$ optical channel matrix is

$$\mathbf{H} = \begin{pmatrix} h_{11} & h_{12} & \cdots & h_{1N_t} \\ h_{21} & h_{22} & \cdots & h_{2N_t} \\ \vdots & \vdots & \ddots & \vdots \\ h_{N_r1} & h_{N_r2} & \cdots & h_{N_rN_t} \end{pmatrix}, \tag{3}$$

where $h_{N_rN_t}$ is the channel DC gain of a directed line-of-sight (LOS) link between the receiver N_r and the transmitter N_t. The LOS link is considered in the system model, because the multipath components are significantly weaker and can thus be neglected. The channel gain can be calculated as follows [3]:

$$h_{\mathrm{N_rN_t}} = \begin{cases} \frac{(\beta+1)A}{2\pi d^2}\cos^{\beta}(\phi)T_s(\psi)g_c(\psi)\cos(\psi), & 0 \le \psi \le \Psi_c \\ 0, & \psi > \Psi_c \end{cases} \tag{4}$$

where $\beta = -\ln 2/\ln(\cos(\Phi_{1/2}))$ and $\Phi_{1/2}$ is the transmitter semiangle. Moreover, A denotes the detector area of the PD and d is the distance between the receiver N_r and the transmitter N_t. The radiant angle and the incident angle are modelled respectively by ϕ and ψ. The optical filter gain T_s and the optical concentrator gain g_c depend on the properties of the receiver.

Thus, optical MIMO signals can be obtained as [13],

$$\mathbf{y} = \mathbf{Hs} + \mathbf{w}, \tag{5}$$

where $\mathbf{y}$ is the N_r-dimensional received vector and $\mathbf{s}$ is the N_t-dimensional transmitted signal vector. In this paper, both N_r and N_t are set to two. In addition, $\mathbf{w}$ is the N_r-dimensional noise vector which is assumed to be real-valued AWGN.

Each PD converts the optical signal to an electrical signal. In this paper, it is assumed that the channel gain is known at the receiver. The ZF detection is used to recover the transmitted symbols as follows,

$$\mathbf{g} = \mathbf{H}^{-1}\mathbf{y}, \tag{6}$$

where $\mathbf{g}$ is an N_t-dimensional vector which contains the estimated transmitted symbols and $\mathbf{H}^{-1}$ denotes the inverse of the channel matrix $\mathbf{H}$. To estimate the indices of the active transmitters, the SM detector compares the values of the elements in $\mathbf{g}$ as follows,

$$\tilde{\mathbf{l}}(k) = \arg\max_{i}(\mathbf{G}(i,k)), i = 1, \cdots, N_t, \tag{7}$$

where $\mathbf{G}$ is the $N_t \times N$ equalized matrix which contains all the estimated transmitted symbols and $\tilde{\mathbf{l}}$ is an N-dimensional vector which contains all the estimated indices. As mentioned, there are two transmitters and two receivers. If $\tilde{\mathbf{l}}(k)$ is equal to one, this means that the symbol received at the time instant k is transmitted from the first LED. Therefore this symbol is a positive-valued OFDM symbol. On the contrary, if the result of $\tilde{\mathbf{l}}(k)$ is two, a negative symbol is transmitted by LED2. As a consequence, the estimated OFDM symbols sequence is

$$\mathbf{x}'(k) = \begin{cases} \mathbf{G}(\tilde{\mathbf{l}}(k), k), & \tilde{\mathbf{l}}(k) = 1, \\ -\mathbf{G}(\tilde{\mathbf{l}}(k), k), & \tilde{\mathbf{l}}(k) = 2. \end{cases} \tag{8}$$

In an ideal scenario, if there is no AWGN, $\mathbf{x}'(k)$ should be the same as $\mathbf{x}(k)$. After recovering the OFDM symbols, $\mathbf{x}'(k)$ is passed through the conventional OFDM demodulation block and the M-QAM demodulator in order to obtain the output bit stream.

IV. Results and Comparisons

This section analyses the spectral efficiency and the BER performance of NDC-OFDM. In addition, this section compares the new technique with DCO-OFDM and ACO-OFDM. Thus, a simple practical optical MIMO channel realized in [13] has been selected for the numerical simulations.

$$\mathbf{H} = 10^{-5} \times \begin{pmatrix} 0.1889 & 0.0713 \\ 0.0713 & 0.1889 \end{pmatrix}, \tag{9}$$

where the values in this matrix describe the path loss between the LEDs and the PDs.

A. NDC-OFDM versus DCO-OFDM

In DCO-OFDM, a DC bias is added and the signal is clipped [9]. In practice, the value of the DC bias, which is related to the average power of the OFDM symbols, is introduced and defined in [6] as

$$B_{\mathrm{DC}} = \alpha\sqrt{\mathrm{E}\{\mathbf{x}^2(k)\}}, \tag{10}$$

where $\mathbf{x}(k)$ is the OFDM symbol frame vector and $10\log_{10}(\alpha^2+1)$ is defined as the bias level in dB. The bias level in the current simulations is set to 7 dB and 13 dB, which are adopted from [6] for consistency. For the simple DCO-OFDM model, signal clipping is used to eliminate the negative part of the DC-biased OFDM symbol frame as,

$$\mathbf{x}_{\mathrm{t}}(k) = \begin{cases} \mathbf{x}(k), & \mathbf{x}(k) \geq 0 \\ 0, & \mathbf{x}(k) < 0 \end{cases} \tag{11}$$

where $\mathbf{x}_{\mathrm{t}}(k)$ is the DC-biased symbol which will be transmitted by an LED.

The spectral efficiencies of NDC-OFDM and DCO-OFDM in an OSM system are defined as,

$$R_{\mathrm{NDC-OFDM}} = \frac{N-2}{2N}\left[\log_2(M_1 N_t) - 1\right] \mathrm{bits/s/Hz}, \tag{12}$$

where N_t is even,

$$R_{\mathrm{DCO-OFDM}} = \frac{N-2}{2N}\log_2(M_2 N_t)\mathrm{bits/s/Hz}, \tag{13}$$

where both M_1 and M_2 are the order of the QAM modulation in NDC-OFDM and DCO-OFDM respectively. From (12) and (13), when $R_{\mathrm{NDC-OFDM}}$ is equal to $R_{\mathrm{DCO-OFDM}}$, the constellation sizes of NDC-OFDM and DCO-OFDM have the following relationship,

$$M_1 = 2M_2. \tag{14}$$

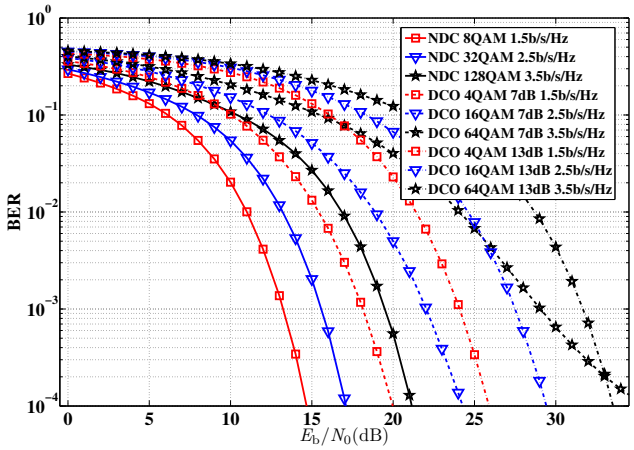

Fig. 3. NDC-OFDM vs. DCO-OFDM with OSM BER performance for the same spectral efficiency

Fig. 3 shows the comparison between NDC-OFDM and DCO-OFDM for the same spectral efficiency, where M_1 = 8, 32, 128 and M_2 = 4, 16, 64. At BER=10^{-4}, the power requirement of NDC-OFDM is at least 5 dB less than the power requirement of DCO-OFDM for all the presented cases in Fig. 3. This indicates that NDC-OFDM can allocate system power more efficiently than DCO-OFDM while maintaining the same spectral efficiency. In DCO-OFDM, signal clipping has a considerable effect on the BER performance when the constellation size is larger than 64. For instance, when using

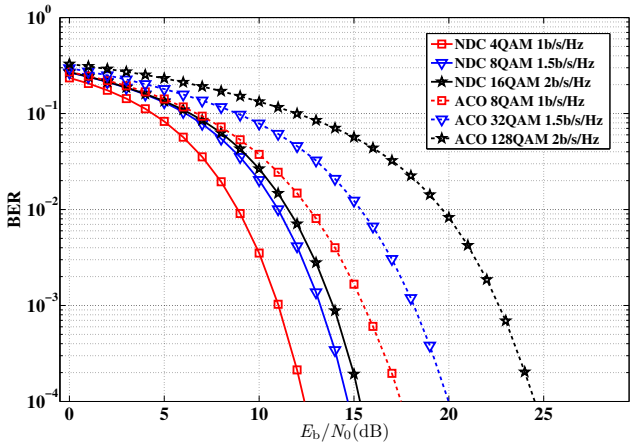

Fig. 4. NDC-OFDM vs. ACO-OFDM with OSM BER performance for the same spectral efficiency

a 7 dB DC-bias and 64-QAM, the nonlinear distortion and the corresponding noise enhancement can be observed in the BER performance after E_b/N_0 reaches 25 dB. As shown in Fig. 3, the BER performance starts exhibiting an error floor. If a larger DC-bias (13 dB) is used in DCO-OFDM, the nonlinear distortion is mitigated, but more power is sacrificed. Since there is no DC-bias and signal clipping from below in NDC-OFDM, it has significant advantages in terms of power efficiency.

B. NDC-OFDM versus ACO-OFDM

As a well-known unipolar optical modulation method, ACO-OFDM has notable energy efficiency at the expense of a reduction in spectral efficiency. In an OSM system, the spectral efficiency of ACO-OFDM is

$$R_{\mathrm{ACO-OFDM}} = \frac{1}{4}\log_2(M_3 N_t)\mathrm{bits/s/Hz}, \qquad (15)$$

where M_3 denotes the order of the constellation. In (12), if the number of OFDM subcarriers is chosen to be large, such as 2048, the formula for the spectral efficiency of NDC-OFDM becomes approximately $\frac{1}{2}\log_2(M_1)$. Thus, in order to compare the BER performance between NDC-OFDM and ACO-OFDM for the same spectral efficiency, M_1 and M_3 should satisfy the following relationship,

$$M_1 = \sqrt{2M_3}. \qquad (16)$$

A BER comparison of NDC-OFDM and ACO-OFDM for the same spectral efficiency is shown in Fig. 4, where $M_1 = 4, 8, 16$ and $M_3 = 8, 32, 128$. It can be seen that NDC-OFDM can use lower order QAM schemes to achieve higher power efficiency than ACO-OFDM. For instance, when $M_1 = 4$ and $M_3 = 8$, NDC-OFDM could save about 5 dB in energy. When $M_1 = 16$ and $M_3 = 128$, ACO-OFDM requires 9 dB higher E_b/N_0 than NDC-OFDM to achieve the same BER performance.

V. Conclusion

In this paper, a novel unipolar modulation method for OWC based on OSM is introduced. Results show that the new approach improves the power efficiency of the OSM-OFDM scheme. For the same spectral efficiency, it exhibits 5 dB to 9 dB higher energy efficiency than the conventional unipolar OFDM technique, ACO-OFDM. When compared to DCO-OFDM, it eliminates the need for a DC-bias. As a consequence, it exhibits a considerable power efficiency gain for the same spectral efficiency.

Acknowledgement

Prof. Haas acknowledges the Engineering and Physical Sciences Research Council (EPSRC) for the support of this work under Established Career Fellowship grant EP/K008757/1.

References

[1] H. Elgala, R. Mesleh, and H. Haas, "Indoor Optical Wireless Communication: Potential and State-of-the-Art," *IEEE Commun. Mag.*, vol. 49, no. 9, pp. 56–62, Sep. 2011, ISSN: 0163-6804.

[2] J. Grubor, S. Randel, K. Langer, and J. Walewski, "Bandwidth Efficient Indoor Optical Wireless Communications with White Light Emitting Diodes," in *In the Proceeding of the 6^{th} International Symposium on Communication Systems, Networks and Digital Signal Processing*, vol. 1, Graz, Austria, Jun. 23–25, 2008, pp. 165–169.

[3] J. M. Kahn and J. R. Barry, "Wireless Infrared Communications," *Proceedings of the IEEE*, vol. 85, no. 2, pp. 265–298, Feb. 1997.

[4] A. Mahdiraji and E. Zahedi, "Comparison of Selected Digital Modulation Schemes (OOK, PPM and DPIM) for Wireless Optical Communications," in *In the Proceeding of the 4^{th} Student Conference on Research and Development (SCOReD 06)*, Jun. 27–28, 2006, pp. 5–10.

[5] J. Armstrong, "OFDM for Optical Communications," *IEEE/OSA Journal on Lightwave Technology (IEEE/OSA JLT)*, vol. 27, no. 3, pp. 189–204, Feb. 2009.

[6] J. Armstrong and B. J. C. Schmidt, "Comparison of Asymmetrically Clipped Optical OFDM and DC-Biased Optical OFDM in AWGN," *Communications Letters, IEEE*, vol. 12, no. 5, pp. 343–345, May 2008.

[7] D. Tsonev, S. Sinanović, and H. Haas, "Novel Unipolar Orthogonal Frequency Division Multiplexing (U-OFDM) for Optical Wireless," in *Proc. of the Vehicular Technology Conference (VTC Spring)*, IEEE. Yokohama, Japan: IEEE, May 6–9 2012.

[8] R. Mesleh, R. Mehmood, H. Elgala, and H. Haas, "An Overview of Indoor OFDM/DMT Optical Wireless Communication Systems," in *7th IEEE, IET International Symposium on Communication Systems, Networks and Digital Signal Processing (CSNDSP)*, Mewcastle, U.K., 21–23 Jul. 2010, pp. 1–5.

[9] S. Dimitrov, S. Sinanovic, and H. Haas, "Clipping Noise in OFDM-based Optical Wireless Communication Systems," *IEEE Transactions on Communications (IEEE TCOM)*, vol. 60, no. 4, pp. 1072–1081, Apr. 2012.

[10] R. Mesleh, H. Haas, C. W. Ahn, and S. Yun, "Spatial Modulation – OFDM," in *Proc. of the International OFDM Workshop*, Hamburg, Germany, Aug. 30–31, 2006.

[11] J. Jeganathan, A. Ghrayeb, and L. Szczecinski, "Spatial Modulation: Optimal Detection and Performance Analysis," *IEEE Communications Letters*, vol. 12, no. 8, pp. 545–547, 2008.

[12] R. Mesleh, H. Elgala, and H. Haas, "Optical Spatial Modulation," *IEEE/OSA Journal of Optical Communications and Networking*, vol. 3, no. 3, pp. 234–244, Mar. 2011, ISSN: 1943-0620.

[13] T. Fath, J. Klaue, and H. Haas, "Coded Spatial Modulation applied to Optical Wireless Communications in Indoor Environments," in *IEEE Proc. of the Wireless Communications and Networking Conference (WCNC)*. Paris, France: IEEE, Apr. 1–4 2012, pp. 1000 – 1004.